

## Analyzing the Effects of Soil-Structure Interactions on the Static Response of Onshore Wind Turbine Foundations Using Finite Element Method

Motallebiyan, A.<sup>1</sup>, Bayat, M.<sup>2\*</sup> and Nadi, B.<sup>2</sup>

<sup>1</sup> M.Sc., Department of Civil Engineering, Najafabad Branch, Islamic Azad University, Najafabad, Iran.

<sup>2</sup> Assistant Professor, Department of Civil Engineering, Najafabad Branch, Islamic Azad University, Najafabad, Iran.

Received: 22 May 2019;

Revised: 01 Mar. 2020;

Accepted: 14 Mar. 2020

**ABSTRACT:** The use of wind turbines to generate electricity has increased in recent years. One of the most important parts of a wind turbine is the foundation, which should be designed accurately because it is influenced by difference forces. Soil cannot carry tension stress; thus, when a wind turbine foundation is applied eccentricity forces, a gap appears between the soil and foundation. The gap will have no positive effect on the ultimate bearing capacity of the foundation. This must be considered when designing the dimensions of an onshore wind turbine on a spread foundation using finite element software in order to avoid error during analysis. In the current study, a spread foundation of an onshore wind turbine was simulated using ABAQUS and PLAXIS-3D software. Based on the results, the effects of Soil-Structure Interaction (SSI), eccentricity of forces, soil strength parameters and the foundation buried depth on static response of the foundation are discussed. The results indicate that the influence of soil-structure interaction is depend on magnitude of eccentricity of forces and depth of foundation, so that soil-structure interaction has little impact on settlement of foundation when eccentricity of forces is less than 1/6 of the diameter of the foundation and this has important effect when the eccentricity forces at an amount exceeding 1/6 of the diameter of the foundation. In addition, this effect decreases with increasing the foundation buried depth and independent of the soil strength parameters ( $\phi'$  and C).

**Keywords:** ABAQUS, PLAXIS, Soil-Structure Interaction, Tension Stress, Wind Turbine Foundations.

### INTRODUCTION

A change in attitude from the use of non-renewable energy resources to renewable energy sources is a global goal. Wind power generation has been the focus of attention in many developed and industrial countries, but

this progress has been huge in countries such as Germany and Denmark (Svensson, 2010). Some countries have set goals for the future use of wind power. The Swedish government has specified a target for the contribution of wind energy of 18% of the total energy produced by 2020. An important aspect of

\* Corresponding author E-mail: bayat.m@pci.iaun.ac.ir

achieving future goals is the repowering of existing wind energy sites. This involves the disassembly of all existing turbines, towers and foundations and replacing them with taller and larger turbines (Lantz et al., 2013). Denmark was the first country to begin replacing wind power projects. This was followed by The Netherlands and Germany (Lantz et al., 2013).

Mortezaie and Rezaie (2018) studied modifying the Performance-Based Plastic Design (PBSD) technique with considering Soil-Structure Interaction (SSI) effects. The result of design show that, involving the interaction effect in PBSD design method, distribution of rebar in beam and columns was changed. However, according to the changes in determining the design base shear, it is expected.

Morshedifard and Eskandari-Ghadi (2017) used a coupled FE-BE method to study the behavior of structures bonded to the surface of a transversely isotropic half-space for considering the effect of time-harmonic sources. Moreover, the effect of SSI on the natural vibration frequency of the structures by using a 3D Finite Element program is also studied. The results indicated that anisotropy of the soil medium can have impressive influence on the dynamic response of the structure and since in natural soil layers. Mohamed et al. (2018) compared the loading capacity of a new foundation solution with an active stabilisation system and a circular raft. The results showed that the load carrying capacity of the cellular raft with active stabilization system is significantly higher than that of the traditional circular raft.

Salmasi et al. (2015) used Seep/W software to analyze the influence of relief wells on a homogeneous earth dam. The results show that total uplift pressure decreases by reducing the distance between relief wells or increasing the diameter of the relief wells. Jamshidi et al. (2018) investigated the effect of spatial variability of

soil parameters on the bearing capacity of the piled raft foundation based on the random field theory using the finite difference software of FLAC3D. The results show that coefficient of variation (COV) of shear strength and its scale of fluctuation were revealed to be the most influential parameters in the stochastic analyses.

Mohamed and Austrell (2017) studied the behavior of three foundation solutions (a traditional raft, a deep raft and a conical raft) for windmills by finite element method using ABAQUS software. The results indicated that using the conical raft result in significantly decrease tilting, the dimensions of the foundation and costs. Cabalar et al. (2016) studied geotechnical and also geophysical properties of the Hasanbeyli area in Turkey. The objective of this research is to develop a generalized technique for foundation design of wind turbine project.

Austin and Jerath (2017) studied effect of SSI on the seismic response of wind turbines by finite element method using ANSYS program. The results indicate that the seismic behaviour of wind turbines is almost independent of the effect of SSI. Bhattacharya et al. (2017) studied the SSI for wind turbines structures under various conditions and summarized the vibration modes of wind turbines structures based on observations from physical modelling tests and numerical study. The results showed that the SSI can be classified based on transfer mechanism and modes of vibration.

Most of the studies mentioned have been done with or without considering the SSI in cases where overturning moments are applied on the foundation and the effect of the SSI on the static behaviour of foundations has not been investigated so far. The current study studied the effect of the SSI on the static response of the onshore wind turbine foundation. For this purpose, the geological and geotechnical properties and the forces effecting the foundation from an onshore

wind turbine that is being constructed near Manjil was used.

### DESIGN LOADS AND SITE CHARACTERISTICS

Iran is a developing country with an abundance of suitable sites for wind energy development. One of the best places for wind turbine development is in northern Iran near the city of Manjil. In 1995 the Iranian governors decided to use renewable energies such as solar power and started to develop several wind farms in Manjil area (Mostafaeipour and Abarghoeei, 2008). Drilling has been done with rotary machines to site investigation. The site investigation operation carried out at Manjil wind farms consisted of drilling 25 boreholes and four test pits. The test pits (4 m in depth with diameters of < 1 m) were drilled to obtain samples for in-place measurement of the soil density and to conduct strength tests. Investigation programs have determined a groundwater level of 27 m and bedrock depth of 30 m from the surface. The site is composed of sedimentary and volcanic rock, with mainly siltstone at 0-15 m and mudstone at 15-30 m. Table 1 indicates the properties of the soil layers after soil mechanics testing on the extracted samples.

In the current study, two types of loads were used to design the turbine foundation:

Serviceability Limit State (SLS) loads and Ultimate Overturning Moment (UOM) loads that are listed in Table 2 (Ishihara et al., 2011; Ishii and Ishihara, 2010; Kawai et al., 2008). SLS loads were used to calculate the settlement and tilting. The UOM loads were used to calculate the required diameter based on the bearing capacity, the sliding resistance and the overturning resistance. The parameters considered in these loads were vertical and horizontal loads (i.e.  $N$  and  $H$ ), bending and twisting moments ( $M$  and  $M_z$ ) that presented in Figure 1a.

### ENGINEERING ANALYSIS AND FOUNDATION DESIGN

The foundation must withstand overturning, sliding and tilting loads by considering the soil bearing capacity and settlement. Calculate the required diameter for the structure load is possible through geotechnical design. In the current study, the diameter of the foundation is obtained based on the soil bearing capacity, overturning, sliding resistances and allowable settlement and then, the largest size of diameter is considered as the foundation diameter (Mohamed and Austrell, 2017). Next, the finite element (FE) model then was used to determine the effects of the SSI. Details of the first stage are presented in the following sections.

**Table 1.** The properties of the soil layers

Description	Depth	Unit weight $\gamma$ (kN/m <sup>3</sup> )	Young's modulus E (kPa)	Internal friction angle $\phi$ (°)	Cohesion C' (kPa)
Silt stone	0-15	19	25000	34	10
Mud stone	15-30	1.4	74800	26	76

**Table 2.** Tower loads, characteristic values

Type of limit state	Loads			
	N (kN)	H (kN)	M (kN.m)	Mz (kN.m)
SLS	2920	555	39300	3850
UOM	2710	765	60500	3030

### Foundation Design for Bearing Capacity

The minimum foundation diameter in this case is obtained based on the bearing capacity of the soil under foundation. In several instances, the moments in two directions are applied on the foundation in addition to the vertical loads, as shown in Figure 1a. In this condition, the contact pressure distribution under the foundation ( $q$ ) is not uniform. Figure 1b shows that, when eccentricity  $e$  equals  $B/6$ ,  $q_{min}$  will equal zero. At  $e > B/6$ ,  $q_{min}$  will be negative (i.e. tension will be produced). Because the soil cannot tolerate tension, separation will occur between the foundation and the underlying soil (Das, 2002). Because the sub-soil under the foundation cannot carry tension, the contact surface between the foundation and soil reduces as the overturning moment loading increases (Mohamed and Austrell, 2017).

In this condition, the surface subjected to compressive load is called the effective foundation surface which is in contact with soil. This surface occurs where the ground stress is assumed to be equally distributed. If the foundation is circular, the effective surface is the elliptic surface as shown in Figure 1c. As shown in Figure 1c, this surface for a circular foundation can be considered as a rectangular surface that originates from an

elliptical area (Mohamed and Austrell, 2017).

To intercept the shear failure mechanism of soil, the maximum stress applied on the base of foundation must not exceeds the allowable bearing capacity of the soil under foundation. Thus, the minimum required diameter of the foundation can be calculated by making the maximum compressive pressure at the base of foundation equal to the allowable bearing capacity of the soil (Mohamed et al., 2018). The maximum compressive pressure at the base of foundation can be calculated as:

$$q_{max} = \frac{V}{b_{eff} l_{eff}} + \frac{6M_t}{b_{eff} l_{eff}^2} \quad (1)$$

where  $V$ : is the sum of the vertical load from the tower, backfill soil and the foundation,  $M_t$ : is the total bending moment,  $b_{eff}$ : is the effective width and  $l_{eff}$ : is the effective length of the foundation (Szerző, 2012).

The effective area for a circular footing (Svensson, 2010) as shown in Figure 1c, can be calculated as:

$$A_{eff} = 2 \left[ R^2 \cos^{-1} \left( \frac{e}{R} \right) - e \sqrt{R^2 - e^2} \right] \quad (2)$$

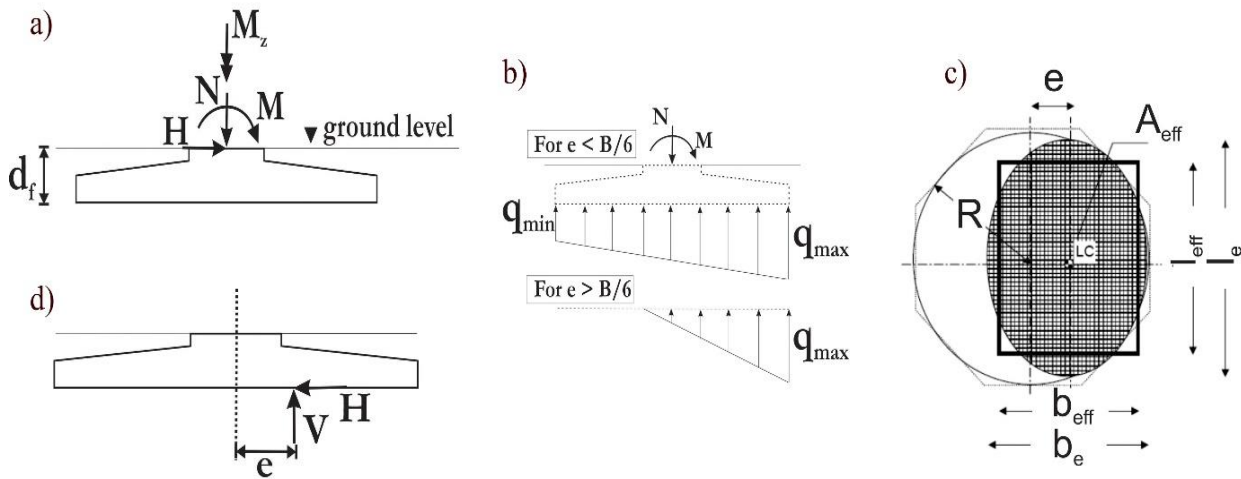


**Fig. 1.** a) Pressure distribution at foundation base with eccentricity; b) Stress distribution under the foundation; c) Effective area for a circular foundation; d) output soil bearing forces (Svensson, 2010)

where  $e$ : is eccentricity (Figure 1d) and  $R$ : is the raft radius ( $R = D/2$ ). Eccentricity  $e$  can be calculated as:

$$e = \frac{M_t}{V} \quad (3)$$

The equivalent rectangular footing of dimensions ( $l_{eff}$  and  $b_{eff}$ ) can be calculated (Mohamed and Austrell, 2017) as:

$$l_{eff} = \sqrt{A_{eff} \frac{R \sqrt{1 - \left(1 - \frac{(R-e)}{R}\right)^2}}{(R-e)}} \quad \text{and} \quad (4)$$

$$b_{eff} = \frac{l_{eff}}{R \sqrt{1 - \left(1 - \frac{(R-e)}{R}\right)^2}} (R - e)$$

The sum of the vertical loads  $V$  and total bending moment  $M_t$  can be calculated as:

$$M_t = M + H \times d_f \quad (5)$$

$$V = N + W_f + W_s - F \quad (6)$$

where  $H$  and  $N$ : are the horizontal and the vertical loads respectively at the tower base,  $M$ : is the bending moment at the tower base,  $W_f$ : is the weight of the foundation,  $W_s$ : is the weight of the backfill,  $d_f$ : is the foundation buried depth as shown in Figure 1a,  $F$ : is the uplift force from groundwater. In Figure 2, these forces are calculated as:

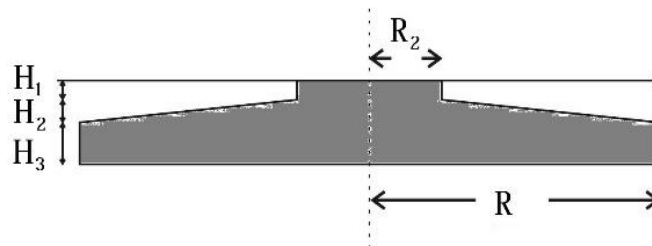


Fig. 2. Geometry of a spread foundation

$$q_{all} = \frac{cN_c S_c d_c i_c g_c b_c + qN_q S_q d_q i_q g_q b_q + 0.5\gamma b_{eff} N_\gamma S_\gamma d_\gamma i_\gamma g_\gamma b_\gamma}{F_s} \quad (10)$$

where  $q_{all}$ : is the allowable bearing capacity of the foundation in kPa, which is calculated by multiplying the effective soil density  $\gamma$  by the foundation base depth  $d_f$ .  $c$ : is cohesion (kPa),  $q$ : is the stress at the foundation level

$$W_f = \pi(R_2^2 \times (H_2 + H_1) + R^2 \times H_3 + \frac{1}{2} \times (R^2 - R_2^2) \times H_2) \times \gamma_c \quad (7)$$

$$W_s = \pi((R^2 - R_2^2) \times H_1 + \frac{1}{2} \times (R^2 - R_2^2) \times H_2) \times \gamma_s \quad (8)$$

$$F = \pi R^2 \gamma_w (d_f - d_w) \quad (9)$$

where  $d_w$ : is the location of the groundwater from the ground surface and  $R$ : is the footing radius. Note that Eq. (7) is valid when the groundwater table,  $d_w$ , is less than the footing base depth. This means that there is no uplift force on the footing if  $d_w > d_f$ .

As mentioned, the minimum diameter of the foundation should be calculated by making the maximum pressure stress under the footing equal to allowable bearing capacity  $q_{all}$  (Mohamed and Austrell, 2017). The  $q_{all}$  value is obtained by separating the theoretical maximum pressure which can be supported without causing shear failure by a safety factor ( $F_s$ ) that equals to 2 to 3 (Bowles, 1997; Terzaghi, 1943).

There are two ways of calculating  $q_{all}$  that depend on the ground conditions (Meyerhof, 1951; Schuppener, 2007; Skempton, 1984). Under drained conditions, Meyerhof's equation can be used to calculate the allowable bearing capacity as:

in kPa,  $\gamma$ : is the effective soil density in  $\text{kN/m}^3$ ,  $N_c$ ,  $N_q$ , and  $N_\gamma$ : are bearing capacity factors which are a function of the internal friction angle,  $S_c$ ,  $S_q$ , and  $S_\gamma$ : are shape factors,  $d_c$ ,  $d_q$ , and  $d_\gamma$ : are depth factors,  $i_c$ ,  $i_q$ , and  $i_\gamma$ :

are load inclination factors,  $g_c$ ,  $g_q$ , and  $g_y$ : are ground inclination factors and  $b_c$ ,  $b_q$ , and  $b_y$ : are base inclination factors. The value of  $q_{all}$  for undrained conditions is:

$$q_{all} = \frac{c_u N_c S_c d_c + q}{FS} \quad (11)$$

where  $c_u$ : is the undrained cohesion,  $N_c$ ,  $S_c$  and  $d_c$ : are the bearing capacity factor, the shape factor and the depth factor, respectively (Skempton, 1984).

In the current study, Eq. (10) was used to calculate the bearing capacity due to groundwater level position which is located in the depth of 27 m from the surface and the soil behaves in a drained manner. The minimum diameter can be calculated by putting the maximum pressure from Eq. (1) as equal to the allowable bearing capacity of the soil from Eq. (10) or (11) as:

$$q_{all} - q_{max} = 0 \quad (12)$$

The minimum diameter of the foundation is found from the equation in an iterative manner, i.e., by assuming a diameter and iterate until the residual of Eq. (12) becomes small enough.

### Foundation Design for Overturning

The resistance against overturning must be considered because wind turbine foundations have high overturning loads (Das, 2002). In order to prevent overturning of a wind turbine under wind loads, the wind load must be balanced by reaction forces from the soil layers under the foundation with eccentricity  $e$  as shown in Figure 1. When  $e$  is equal to raft radius  $R$ , the limiting case occurs theoretically and stability moment  $M_s$  is calculated as:

$$M_s = V \times R \quad (13)$$

Interception of overturning is a method of defining the safety factor against overturning

as  $F_s \geq 1.5$  with respect to  $M_s$  (Morgan and Ntambakwa, 2008). In this case,  $F_s$  is equal to:

$$F_s = \frac{M_s}{M_t} \quad (14)$$

Szerző (2012) suggested focusing on eccentricity  $e$ , which should comply with:

$$e = \frac{M_t}{V} \leq 0.25R \text{ for service loads and } \leq 0.58R \text{ for ultimate loads} \quad (15)$$

where  $R$ : is the raft radius ( $R = D/2$ ),  $V$ : is the sum of vertical loads and  $M_t$ : is the sum of the total bending moment (Szerző, 2012).

According to the requirements of overturning, the diameters of the footings are calculated by Eqs. (14) and (15) with  $F_s = 1.5$  and  $e = 0.58 R$ . Total bending moment  $M_t$  can be calculated using Eq. (5), the sum of the vertical loads  $V$  and stability moment  $M_s$  can be obtained by using Eqs. (6) and (13), respectively.

By assuming a diameter and iterate for the residuals of Eqs. (14) and (15), the diameter of the foundation can be calculated using the equation in an iterative manner. The required diameters are the largest values obtained from Eqs. (14) and (15) (Mohamed and Austrell, 2017).

### Foundation Design for Settlement

The minimum foundation diameter in this case is calculated by considering the settlement of the foundation. In the current study, the allowable differential settlement and the maximum settlement of the foundation are assumed 3 mm/m and 50 mm, respectively. Because of groundwater level is located in the depth of 27 m from the surface we should use the theory of elasticity to determine elastic settlement of shallow foundations. The maximum settlement under the foundation can be calculated as (Das,

2007):

$$S_e = q(\alpha B') \frac{1 - \vartheta^2}{E} I_s I_f \quad (16)$$

where  $q$ : is net applied stress at the level of the foundation,  $\alpha$ : is a factor depending on the location of the foundation where settlement is being calculated,  $B'$ : is the width of foundation,  $E$ : is the elastic modulus of soil,  $\vartheta$ : is Poisson's ratio for the undrained condition,  $I_s$  and  $I_f$ : are shape and depth factors respectively.

### FINITE ELEMENT MODEL

In the current study, all numerical finite element simulations were performed in ABAQUS 6.12 and PLAXIS-3D Foundation 1.6. The details of the modeling approaches are presented below.

#### Modeling in ABAQUS Software

In the current study, an elastic perfectly-plastic constitutive model along with the Mohr-Coulomb failure criterion were selected to simulate the soil layers, similar previous studies (Niels and Matti, 2005; Potts and Zdravkovic, 1999). A fine-grid mesh surrounded the foundation and a coarse-grid mesh was used for the far field. As shown in Figure 3a, to prevent the influence of boundary conditions of the soil on the results, the mesh boundaries extended 40 m from the edge of the raft foundation. The depth of the soil was determined by the bedrock depth in the wind farms in Manjil which is 30 m below

the surface of the soil. To increase safety factor and the possibility of flooding on the site, foundation was simulated on the soil. An 8-node brick, reduced integration element (C3D8R) was selected to model the foundation, soil and steel ring. The parameter values of the mesh are shown in Figure 3a for 29,568 elements and 34,386 nodes for the soil.

Table 2 shows the values of applying the loads include loads and moment to the turbine foundation. Figure 3b shows the mesh and the dimensions of the designed foundation, which is circular with a diameter of 20 m and height of 3 m.

The foundation was modeled as linearly elastic 3D structures. Figure 3b also shows the dimensions of the steel ring embedded in the foundation. The properties of the soil, steel ring and foundation concrete used in the FE model are given in Table 3. To measure the effect of foundation depth on the results, the foundation was simulated in ABAQUS at depths of 0, 3, 6 and 9 m.

As previously mentioned, when the extremely high overturning moment is applied on the wind turbine foundation results in partial separation of the foundation from the soil that has important effect on the behavior of the foundation. Several types of FE software, including PLAXIS-3D and 2D, consider this interaction under static loading and the nodes in the contact area between the foundation and soil are common with no possibility of separation between them. Therefore, the soil is simulated with the ability to carry tension stress which is contrary to reality.

Table 3. Material properties

Description	Unit weight $\gamma$ (kN/m <sup>3</sup> )	Young's modulus E (kPa)	Internal friction angle $\phi$ (°)	Cohesion C' (kPa)	$\Psi$ (°)	Poisson's ratio $\vartheta$
Soil properties	19	25000	34	10	4	0.35
Concrete properties	25.5	20.59×10 <sup>6</sup>	-	-	-	0.2
Steel properties	78.5	210×10 <sup>6</sup>	-	-	-	0.3

ABAQUS is able to model the partial separation of the foundation from the soil with normal behavior using the restriction enforcement technique and pressure overclosure as the hard contact, allowing separation. The horizontal forces from the wind-load can cause sliding; thus, a surface-to-surface contact was created between soil and foundation in ABAQUS, so that the “tangential behavior” with a friction coefficient of 0.3 has been defined as properties of the contact. The interaction of the embedded region was defined between the steel ring and the concrete. The soil nodes of the boundary surrounding the model were fixed in the horizontal direction; however, the nodes at the bottom boundary of the finite element model were fixed.

Three steps were used in deformation analysis. The first was the geostatic step to ensure that equilibrium due to soil weight was satisfied in the soil. The second was the static general step to set the foundation on the soil. The third was the static general step to apply the tower loads as shown in Table 2.

### **Modeling in PLAXIS-3D Software**

The Finite Element software PLAXIS-3D Foundation 1.6 (Brinkgreve et al., 2012) was used for simulation modeling. It is a Finite Element software for analyzing soil and rock, especially developed for analyzing stability and deformation in geotechnical engineering. Ten-node tetrahedral elements were utilized to generate the finite element models of the soil and foundation. Interface elements were used between both the soil layer and the foundation soil.

Figure 4a shows a PLAXIS-3D model with its geometrical properties. To prevent the influence of boundary conditions defined for the soil on the results, mesh boundaries extended out 40 m from the edge of the raft foundation and the depth of the soil was determined as the depth at bedrock as 30 m.

Displacement of the model boundaries (bottom and all peripheries, plus normal directions in symmetry) were fixed in all directions. The soil characteristics are also summarized in Table 3.

PLAXIS-3D is unable to simulate the dimensions of the designed foundation with a sloping surface as shown Figure 3c. In the current study, the foundation was simulated as stairway concrete foundation in PLAXIS-3D (see Figure 4b). The foundation was modeled as a linearly elastic 3D structure with the concrete properties given in Table 3. The numerical analyses were done in several computational phases. The initial geometry configuration and stress states have been considered in the initial phase. The second phase was for design of the foundation on the soil and phase three was for the tower loads (Table 2).

## **RESULTS AND DISCUSSION**

In this section, the results of the software analysis on the two examples defined in the previous section will be displayed.

### **Maximum Settlement**

It is not possible to consider the partial separation of the foundation from the soil when the SSI is not considered, which can have an important effect on the maximum settlement. If the SSI in ABAQUS is considered, the maximum settlement under the SLS loads for a foundation with a diameter of 20 m on a siltstone layer is 3.13 cm. However, when this contact is not considered in ABAQUS, the maximum settlement is 3.06 cm. Also, the maximum settlement under SLS loads in PLAXIS-3D for a foundation with a diameter of 20 m on a siltstone layer is 3.03 cm.

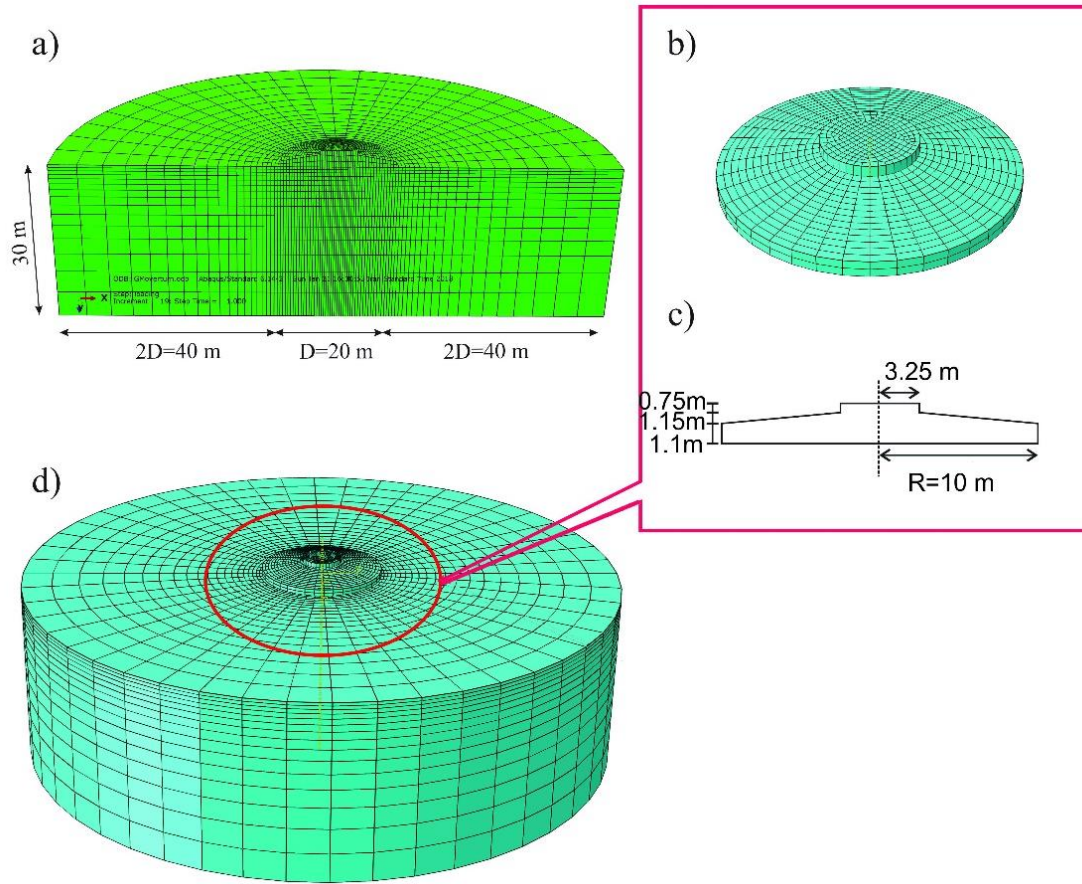


**Fig. 3.** a) Three dimensional Finite Element model of the soil; b) Three dimensional Finite Element model of foundation; c) Dimensions of the spread foundation; d) Finite Element model of soil foundation interaction

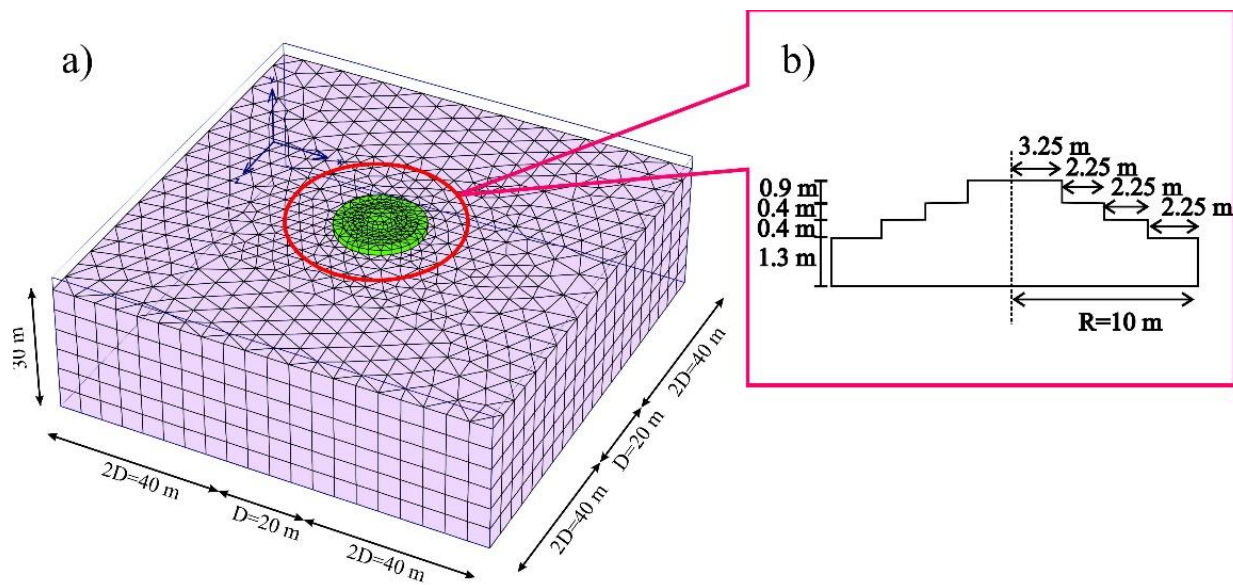


**Fig. 4.** a) Three dimensional finite element model of the soil and foundation in Plaxis-3D; b) Detailed Dimensions of the spread foundation in Plaxis-3D

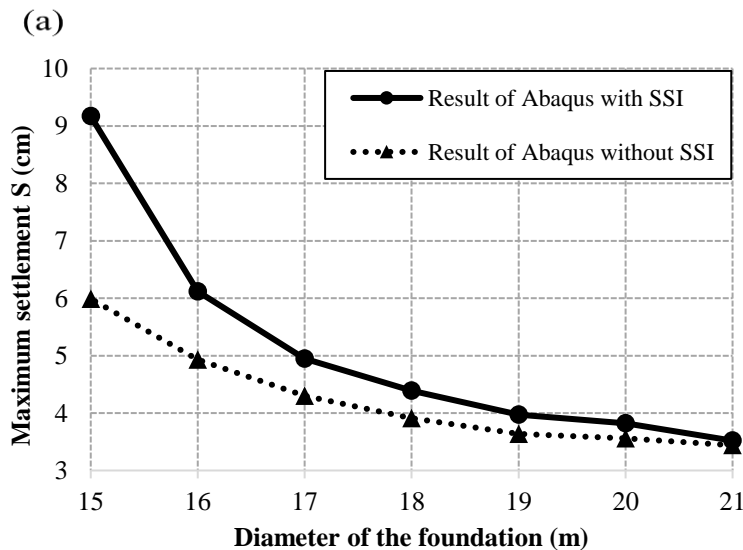
In addition, the maximum settlement under UOM loads for the foundation is 3.81 cm with considering the SSI in ABAQUS. In contrast, the maximum settlement is 3.62 cm when the SSI is not considered. Also, the maximum settlement due to UOM in PLAXIS-3D for similar condition is 3.59 cm. As can be seen, when there is no gap between the foundation and soil in ABAQUS, the maximum settlement obtained by ABAQUS and PLAXIS-3D are mostly equal. The difference in these results is a function of the foundation diameter.

Figure 5a shows the effect of the foundation diameter on the maximum settlement. As shown in the figure, the difference between the results of maximum settlement increased with a decrease of the diameter. The difference between the results of the two methods versus  $e/D$  is shown in Figure 5b. The results indicate that the difference is not significant when  $e/D$  is less than  $1/6$  and foundation does not separate from the soil and so uplift does not occur. However, for  $e/D$  greater than  $1/6$ , the difference between the results increases significantly. Table 4 shows the results from simplified calculation method by using Eqs. (1-16) respectively to verify the accuracy of the FE results. In order to use Eq. (16),

triangular load convert to equivalent uniform rectangular load. As can be seen, the maximum settlement obtained by ABAQUS with considering the SSI are equal the calculations.

The maximum settlements obtained from ABAQUS and PLAXIS-3D by modeling a foundation with a diameter of 20 m at different depths on siltstone and mudstone layers are shown in Figures 6a,b, respectively. The results indicate that the difference between the results is reduced due to increasing of the embedded depth of the foundations. The effects of cohesion and internal friction angle of the soil on the difference in the maximum settlement under UOM loads in the two modes for a siltstone layer as a function of depths are shown in Figures 7 and 8, respectively.

As shown in Figure 7, the maximum settlement is almost independent of soil cohesion and the difference in the maximum settlement in the two modes at a depth of 3 m is more impressive than that in the other depths (i.e. 0 and 9 m), while the results presented in Figure 8 show that the angle change of 20 to 30 has an important effect on the maximum settlement at ground level. Here, too, the greatest difference observed at a depth of 3 m



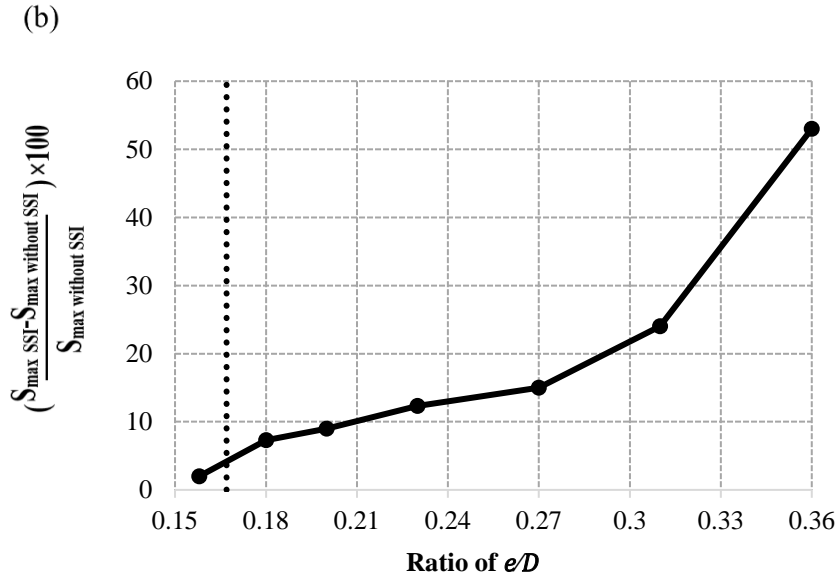
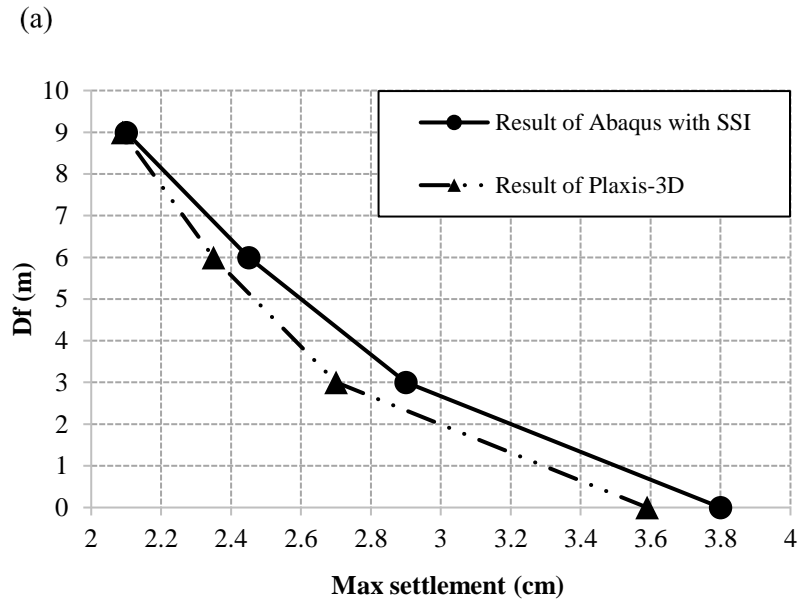
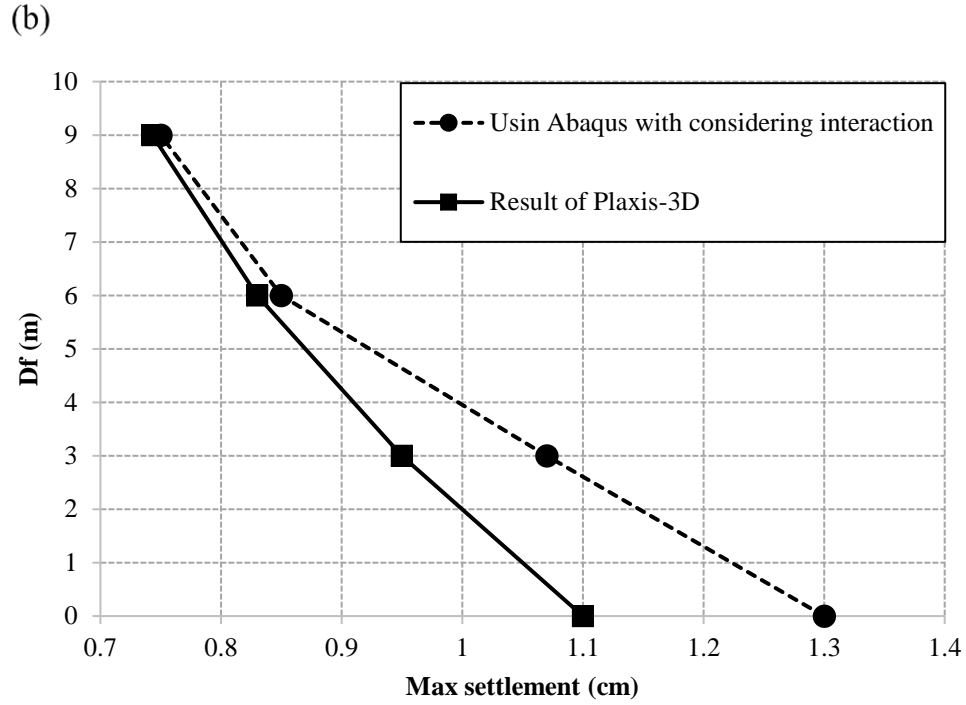


Fig. 5. a) Effect of the foundation diameter on the maximum settlement; b) The difference between the results of the two methods (with or without considering the SSI) versus  $e/D$

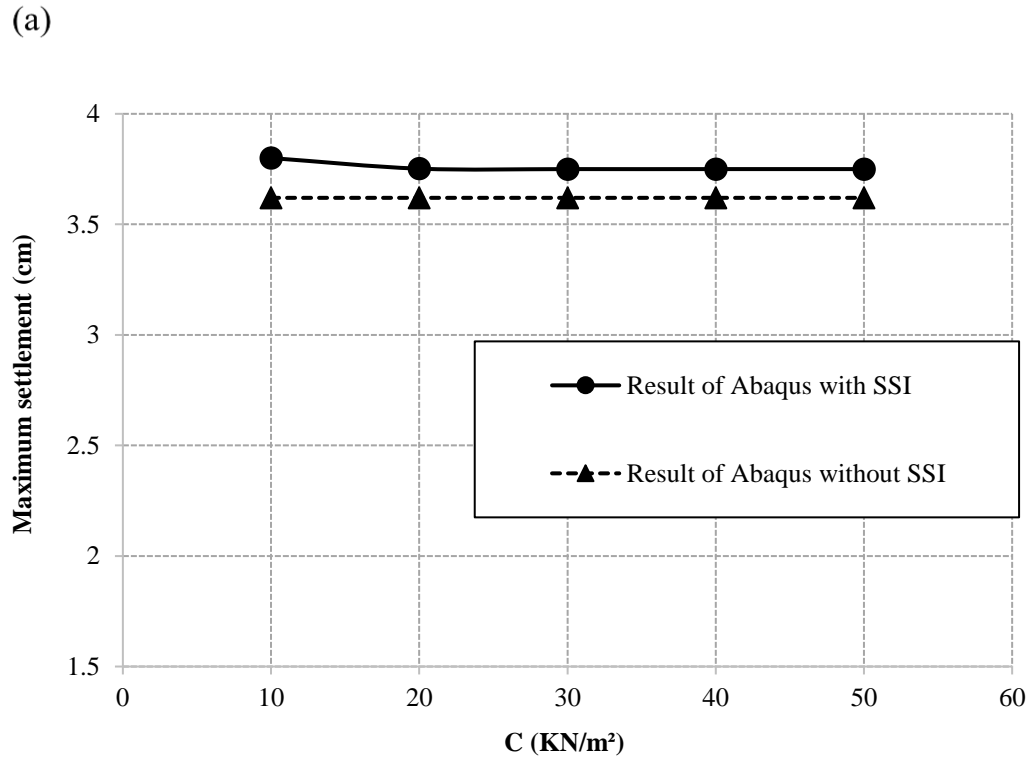
Table 4. Results of simplified calculation method

layer	loads	D	$d_f$	$W_f$ (kN)	$M_t$ (kN)	$V$ (kN)	$e$	$b_{eff}$ (m)	$q_{max}$ (kPa)	FS $\geq$ 1.5	$S_e$ (cm)
Silt stone	UOM	21	0	15907	60500	18617	3.2	12.4	188	3.23	3.6
		20	0	14532	60500	17242	3.5	11.1	226	2.85	3.8
		19	0	13224	60500	15934	3.8	9.7	283	2.5	4.2
		18	0	11984	60500	14694	4.1	8.3	372	2.2	4.7
		17	0	10810	60500	13520	4.5	6.8	528	1.9	5.5
		16	0	9704	60500	12414	4.9	5.2	842	1.6	6.7
		15	0	8664	60500	11374	5.3	3.6	1659	1.4	9.2

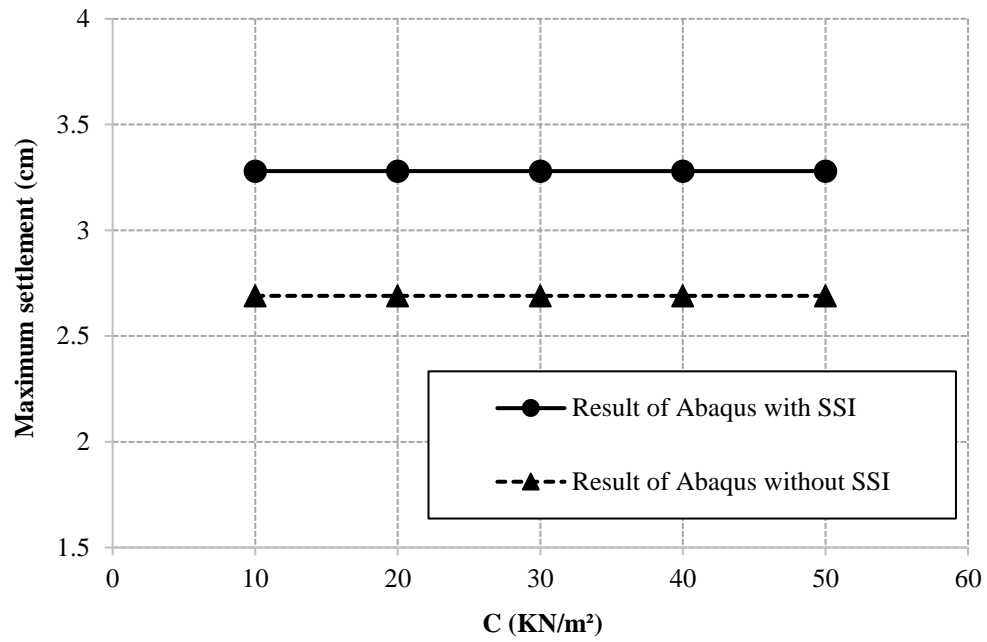




**Fig. 6.** a) The maximum settlements obtained from ABAQUS and PLAXIS-3D by modeling a foundation on siltstone layers; b) The maximum settlements obtained from ABAQUS and PLAXIS-3D by modeling a foundation on mudstone layers.



(b)



(c)

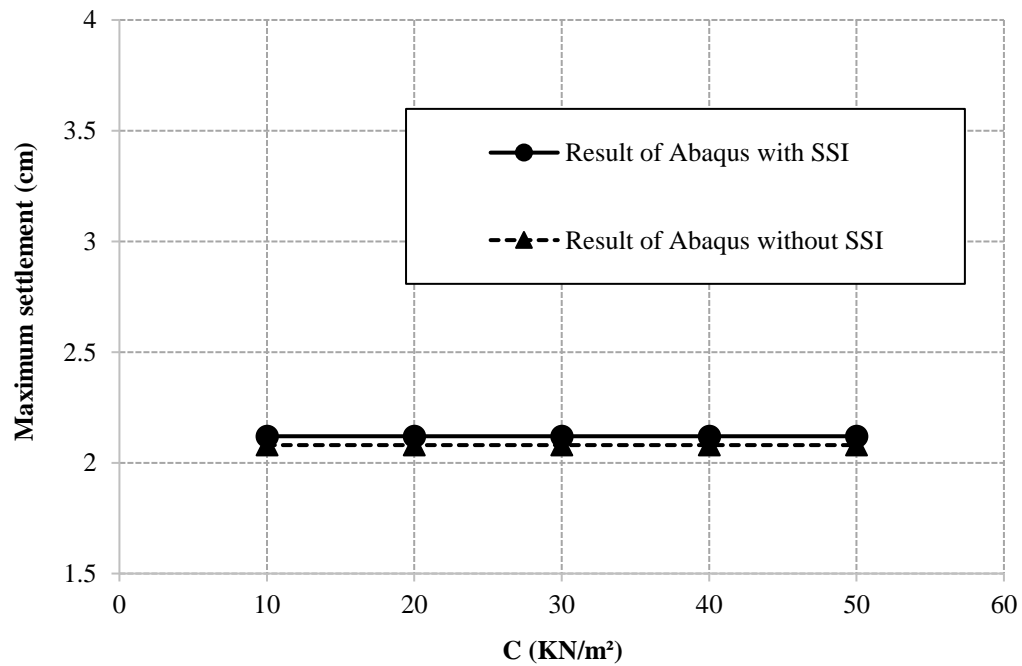
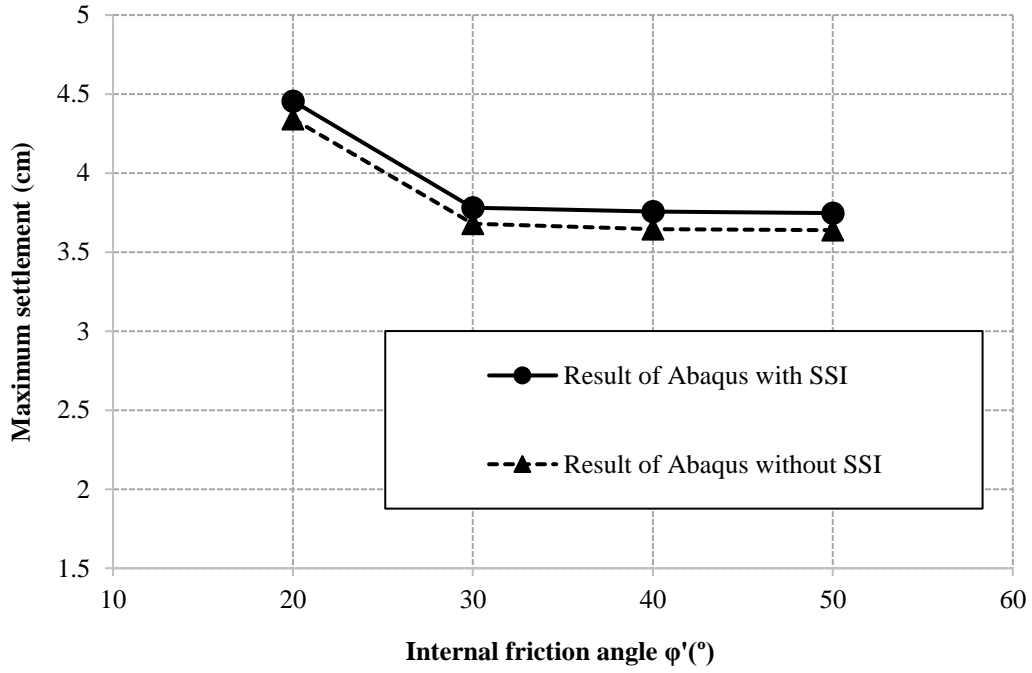
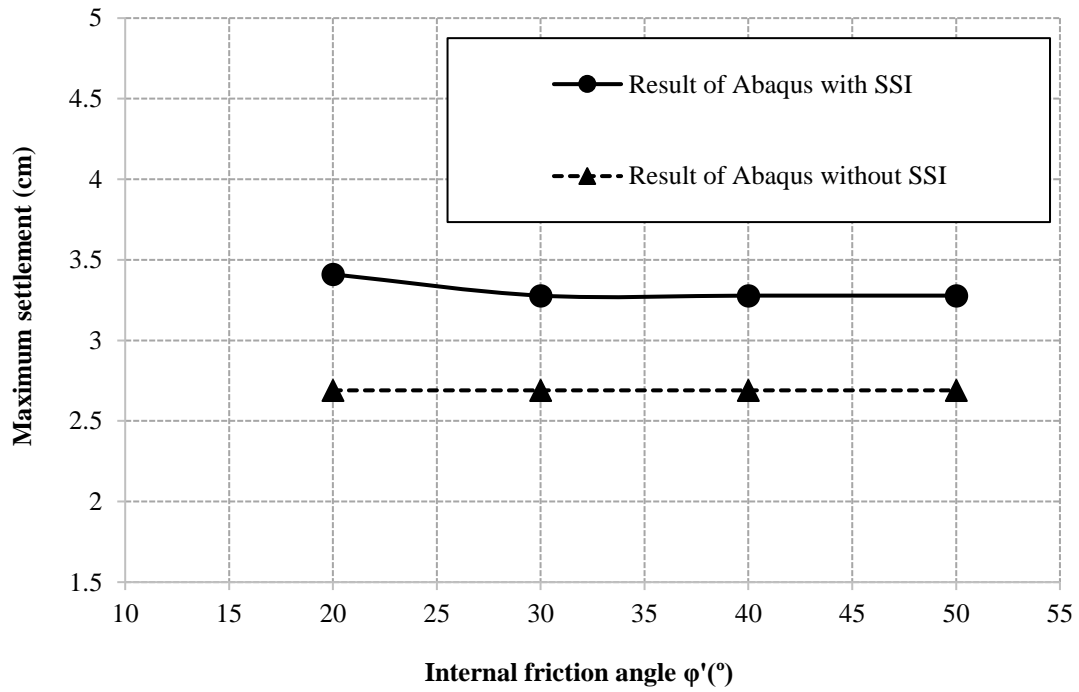


Fig. 7. The effects of cohesion on the difference in the maximum settlement under UOM loads for a siltstone layer as a function of depths at the depth of: a) 0 meter; b) 3 meter; c) 9 meter

(a)



(b)



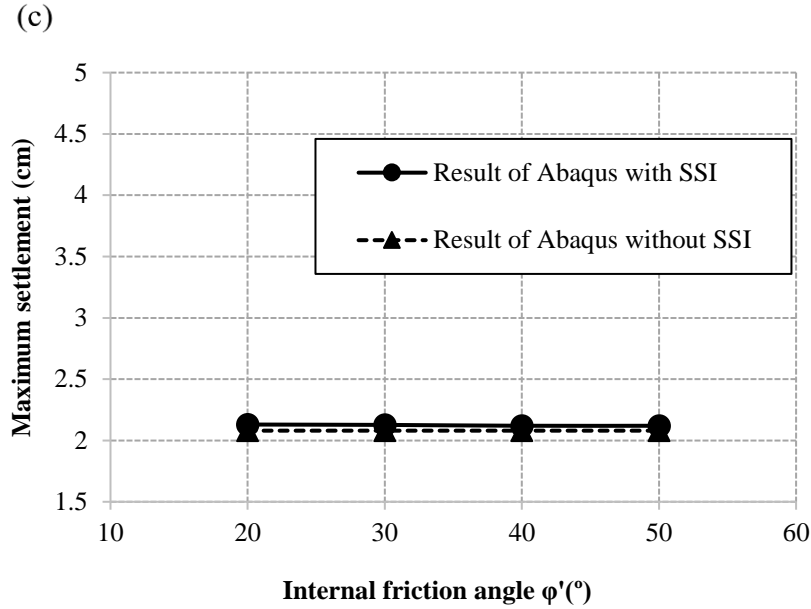


**Fig. 8.** The effects of internal friction angle on the difference in the maximum settlement under UOM loads for a siltstone layer as a function of depths at the depth of: a) 0 meter; b) 3 meter; c) 9 meter

### Stress under the Foundation

Generally, it is accepted that soil layers are not capable of resisting significant tensile forces. For this reason, when the ultimate overturning loads applied the foundation and  $e/D$  exceeds  $1/6$ , these loads will cause a gap between the foundation and the supporting soil. Under these conditions, the vertical stress in the gap becomes zero. Figure 9

shows the amount of vertical stress under a foundation with a diameter of 20m along a line between the maximum and the minimum settlement. As shown in the results, the value of vertical stress along the edge of the foundation (point A) to an approximate distance of 3.5 m was zero, when the SSI was defined. This indicates that the foundation has been separated from the supporting soil.

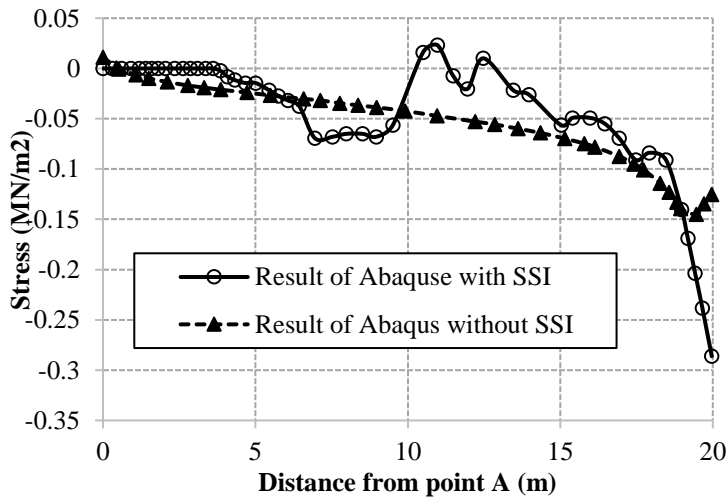


**Fig. 9.** The amount of vertical stress under the foundation with a diameter of 20 m using line AB between the maximum and the minimum settlement

The results obtained from modeling the same foundation without defining the SSI is shown also in Figure 9. The tensile stress can be observed even at point A. In this condition, the foundation has not been separated from the supporting soil, because the SSI has not been defined. When  $e/D$  exceeds  $1/6$ , the UOM loads lead to upward movement of the foundation that result in tensile stress on the part of the supporting soil area.

## CONCLUSIONS

The current study examined the effect of SSI on the static response of onshore wind turbine foundations and compared the maximum settlement obtained by ABAQUS and PLAXIS-3D. The results of FE analysis indicate that SSI has important effect on the maximum settlement and stress distribution under the foundation. The results show that when in FE software, a spread turbine foundation is applied eccentricity forces, if  $e/D$  is less than  $1/6$ , the SSI has not effect on the difference of maximum settlement; however, when  $e/D$  exceeds  $1/6$  (with decreasing the diameter of foundation), a part of the foundation base area will be subjected to tension stresses; thus, the difference in maximum settlement increases.

Under these conditions, the vertical stress in the gap becomes zero when the SSI was defined but the results obtained from modeling the same foundation without defining the SSI indicated that tensile stress on the part of the supporting soil area can be observed and the existence of tensile stress under the foundation was the cause of the error in the results. The results also showed that, when the depth of the foundation increased in response to the growing overhead force, the difference in maximum settlement decreased; however, the cohesion and friction angle of the soil had no effect on the difference in the results of maximum settlement.

According to the results when there is no gap between the foundation and soil in ABAQUS, the maximum settlement obtained by ABAQUS and PLAXIS-3D are mostly equal. Because FE software such as PLAXIS-3D and 2D are unable to define the SSI and cannot simulate the behavior of the foundation and soil when  $e/D$  exceeds  $1/6$  as well as is possible in ABAQUS.

## REFERENCES

- Austin, S. and Jerath, S. (2017). "Effect of soil-foundation-structure interaction on the seismic response of wind turbines", *Ain Shams Engineering Journal*, 8(3), 323–331.
- Bhattacharya, S., Nikitas, G., Arany, L. and Nikitas, N. (2017). "Soil-Structure Interactions (SSI) for offshore wind turbines", *The Institution of Engineering and Technology*, 24(16), 1-23.
- Bowles, L. (1997). *Foundation analysis and design*, McGraw-hill.
- Brinkgreve, R.B.J., Engin, E. and Swolfs, W.M. (2012). "Plaxis 3D 2012", Plaxis bv, the Netherlands.
- Cabalar, A.F., Uyan, R.S. and Akbulut, N. (2016). "A Study of Foundation Design for Wind Turbines in Hasanbeyli, Turkey", *Soil Mechanics and Foundation Engineering*, 53(5), 298-303.
- Das, B.M. (2002). *Principles of Foundation Engineering*, McGraw-Hill handbooks.
- Ishihara, T., Ishii, H. and Nishio, M. (2011). *Maximum wind loads on a wind turbine under operating conditions*, European Wind Energy Association: Europe's Premier Wind Energy Event.
- Ishii, H. and Ishihara, T. (2010). "Numerical study of maximum wind load on wind turbine towers under operating conditions", *The Fifth International Symposium on Computational Wind Engineering (CWE2010)*, Chapel Hill, North Carolina, USA, May 23-27, pp. 1-8
- Jamshidi Chenari, R., Ghorbani, A., Eslami, A. and Mirabbasi, F. (2018). "Behavior of piled raft foundation on heterogeneous clay deposits using random field theory", *Civil Engineering Infrastructures Journal*, 51(1), 35-54.
- Kawai, H., Michishita, K. and Deguchi, A. (2008). "Design wind loads on a wind turbine for strong wind", *Proceedings of the BBAA VI International Colloquium on: Bluff Bodies Aerodynamics and Applications*, Milano, Italy, Vol. 2024.
- Lantz, E., Leventhal, M. and Baring-Gould, I. (2013). *Wind power project repowering: Financial*

- feasibility, decision drivers, and supply chain effects*, National Renewable Energy Laboratory (NREL).
- Meyerhof, G.G. (1951). "The ultimate bearing capacity of foundations", *Geotechnique*, 2(4), 301-332.
- Mohamed, W. and Austrell, P.E. (2017). "A comparative study of three onshore wind turbine foundation solutions", *Computers and Geotechnics*, 94, 46-57.
- Mohamed, W., Austrell, P.E. and Dahlblom, O. (2018). "A new and reusable foundation solution for onshore windmills", *Computers and Geotechnics*, 99(February), 14-30.
- Morgan, K. and Ntambakwa, E. (2008). "Wind turbine foundation behavior and design considerations", *Proceedings of the American Wind Energy Association Windpower Conference*, Houston, Texas.
- Morshedifard, A. and Eskandari-Ghadi, M. (2017). "Coupled BE-FE scheme for three-dimensional dynamic interaction of a transversely isotropic half-space with a flexible structure", *Civil Engineering Infrastructures Journal*, 50(1), 95-118.
- Mortezaie, H. and Rezaie, F. (2018). "Seismic behavior and dissipated plastic energy of performance-based-designed high-rise concrete structures with considering soil–structure interaction effect", *Civil Engineering Infrastructures Journal*, 51(1), 199-215.
- Mostafaeipour, A. and Abarghooei, H. (2008). "Harnessing wind energy at Manjil area located in north of Iran", *Renewable and Sustainable Energy Reviews*, 12(6), 1758-1766.
- Niels, S.O. and Matti, R. (2005). *The mechanics of constitutive modeling*, Elsevier.
- Potts, D. and Zdravkovic, L. (1999). *Finite Element analysis in geotechnical engineering: Application*, Vol. 1, Thomas Telford.
- Ripa Alonso, T. and González Dueñas, E. (2014). "Cracks analysis in onshore wind turbine foundations", *IABSE Symposium Report*, 102(23), 1086-1092.
- Salmasi, F., Mansuri, B. and Raufi, A. (2015). "Use of numerical simulation to measure the effect of relief wells for decreasing uplift in a homogeneous earth dam", *Civil Engineering Infrastructures Journal*, 48(1), 35-45.
- Schuppener, B. (2007). "Eurocode 7: Geotechnical design, Part 1: General rules-its implementation in the European member states", *Proceedings of the 14<sup>th</sup> European Conference on Soil Mechanics and Geotechnical Engineering*, Madrid, Spain, 24-27 September, 2, 279-289.
- Svensson, H. (2010). "Design of foundations for wind turbines", M.Sc. Dissertation, Lund University.
- Szerző, Á. (2012). "Optimization of foundation solutions for wind turbines", *Mathematical Modeling in Civil Engineering*, 4, 215-225.
- Terzaghi, K. (1951). *Theoretical soil mechanics*, JohnWiley & Sons, New York, 11-15.